PERIODICALLY FULLY DEVELOPED LAMINAR FLOW AND HEAT TRANSFER IN A TWO-DIMENSIONAL HORIZONTAL CHANNEL WITH STAGGERED FINS

Oğuz TURGUT[1,*] and Kamil ARSLAN[2]

[1]Gazi University, Faculty of Engineering, Department of Mechanical Engineering and Clean Energy Research and Application Center (TEMENAR), Maltepe-Ankara, Turkey
[2]Karabük University, Faculty of Engineering, Department of Mechanical Engineering, Karabük, Turkey

Two-dimensional periodically fully developed laminar forced convection fluid flow and heat transfer characteristics in a horizontal channel with staggered fins are investigated numerically under constant wall heat flux boundary condition. Study is performed using ANSYS Fluent 6.3.26 which uses finite volume method. Air (Pr ≅ 0.7) and Freon-12 (Pr ≅ 3.5) are used as working fluids. Effects of Reynolds number, Prandtl number, fin height, and distances between two fins on heat transfer and friction factor are examined. Results are given in the form of non-dimensional average Nusselt number and average Darcy friction factor as a function of Reynolds number for different fin distances and Prandtl numbers. The velocity and temperature profiles are also obtained. It is seen that as the fin distance increases, behavior approaches the finless channel, as expected. Also, thermal enhancement factors are given graphically for working fluids. It is seen that heat transfer dominates the friction as both the distance between two fins and Prandtl number increase. It is also seen that fins having blockage ratio of 0.10 in two dimensional periodically fully developed laminar flow is not advantageous in comparison to smooth channel without fins.

Key words: *laminar flow, heat transfer, parallel plate channel, fin, periodic flow, ANSYS Fluent*

1. Introduction

Many compact heat exchangers operate in the laminar flow regime owing to small velocities and passage sizes. In addition, the passage lengths are too long. Hence, the flow is fully developed over much of the duct's length.

The laminar flow and heat transfer characteristics in two-dimensional channels with baffles or fins have been studied by many investigators. The investigation of forced convection in the two-dimensional duct attracts much interest due to its wide applications in many industrial systems, such as heat exchangers, nuclear reactors and electronic cooling systems. To increase the heat transfer rates over the laminar fully developed values, devices such as ribs, fins or baffles that interrupt the development of the boundary layers are usually placed on the channel walls with in-line or staggered arrangement.

When two series of fins are placed on the respective walls of a channel, the flow is expected to reach a periodic fully developed character after a short entrance length [1, 2]. A comprehensive review of laminar flow results up to the eighties was performed by Shah and London [3]. Webb and Ramadhyani [4] carried out numerical investigation of laminar forced convection conjugate heat transfer in two parallel plates mounted baffles on the surfaces with staggered arrangement. Constant heat flux boundary condition was applied on the top and bottom surfaces of the parallel plates. Periodically fully developed flow condition was observed in the channel. Different Reynolds numbers, Prandtl numbers and geometries were investigated. Kelkar and Patankar [5] investigated numerically the flow and heat transfer in two parallel plates mounted baffles with staggered arrangement on the surfaces under constant wall temperature condition. It was observed that periodic flow condition was

[*]Corresponding author e-mail: oturgut@gazi.edu.tr

obtained in the channel at a certain distance from inlet of the channel. Lazaridis [6] investigated the heat transfer in a parallel plate channel with staggered fins. An equation was generated from data of Kelkar and Patankar [5]. Cheng and Huang [7] investigated numerically laminar forced flow in two parallel plates having fins with staggered arrangement. The channel walls are kept at uniform but different surface temperatures. Velocity and temperature distributions of the periodically fully-developed flow were examined through a stream function-vorticity method with a finite difference scheme. Based on the obtained solutions of flow field, the effect of Reynolds number and other geometric parameters on the heat transfer coefficient and the friction factor were evaluated. Luy *et al*. [8] conducted a two-dimensional numerical study to investigate the effect of series of fins, mounted on the bottom wall, on laminar fluid flow and heat transfer. Two walls are kept at constant temperature but unequal temperature. Kim and Anand [9] studied numerically the laminar fully developing flow condition in the two parallel plates mounted blocks on the surfaces. Surfaces were isolated, and heat generating blocks were placed in the channel. Numerical investigation was conducted for different Reynolds numbers, block heights, thicknesses of the blocks, and thermal conductivities of the blocks. Wang *et al*. [10] examined numerically heat transfer for unsteady flow in parallel plates mounted fins with staggered and in-line arrangements. Yuan *et al*. [11] carried out a numerical study for the periodically fully-developed flow in two dimensional channels with streamwise-periodic round disturbances on its two walls. Tehrani and Abadi [12] investigated numerically laminar flow and heat transfer in the entrance region of a two dimensional horizontal channel, with in-line ribs, for constant surface temperature boundary condition. Results were obtained for the Reynolds numbers ranging from 100 to 500, Prandtl number of 0.7, and different blockage rates ranging between 0.1 and 0.3. It was reported that periodically fully developed condition for air takes place after the third to the sixth rib depending on the Reynolds number. Mousavi and Hooman [13] numerically investigated two dimensional laminar fluid flow and heat transfer in the entrance region of a channel with staggered baffles at constant temperature boundary condition for Reynolds numbers between 50 and 500 and baffle heights ranging from 0 and 0.75. Onur *et al*. [14] conducted two-dimensional numerical analysis of laminar forced convection fluid flow and heat transfer between two isothermal parallel plates with baffles. Baffles were placed in staggered arrangement in the channel. The effect of the number of baffle and Reynolds number on flow and heat transfer was examined for hydrodynamically fully developed and thermally developing flow. It has been seen that the number of baffles and Reynolds number have important effect on flow and heat transfer. Results have also shown that increase in the Reynolds number and baffle number causes an increase in average Nusselt number and friction factor. Sripattanapipat and Promvonge [15] presented a numerical study of two-dimensional laminar periodic flow in a channel containing staggered diamond shaped baffles. Turan and Oztop [16] analyzed two-dimensional laminar flow in a channel containing cutting edged disc using finite volume technique. Xia *et al*. [17] numerically studied periodically fully developed laminar flow in parallel plate channel for three groups of crescent-shape protrusions. Garg *et al*. [18] numerically investigated two dimensional laminar flow and heat transfer in a channel having diamond-shaped baffles. Turgut and Kizilirmak [19] conducted a numerical study to investigate the turbulent flow and heat transfer in a circular pipe with baffles. It was reported that the flow shows periodic behavior after a certain baffle.

Literature survey showed that most of the investigations stated above investigated the entrance region problem for air at constant temperature boundary condition. However, different behavior is anticipated when Prandtl number is greater than unity. Also, boundary condition affects the heat transfer performance in laminar flow. Therefore, in this study, periodically fully developed forced convection laminar flow and heat transfer characteristics in a two-dimensional horizontal channel mounted fins on the surfaces with staggered arrangements have been investigated numerically at constant wall heat flux boundary condition. ANSYS Fluent 6.3.26 commercial code is used for numerical study. This investigation has been carried out for seven different Reynolds numbers ($100 \leq Re \leq 500$), two different Prandtl numbers (0.7 and 3.5), one fin height ($F/H = 0.10$) and the special case of finless state ($F/H = 0$), and five different distances between two fins ($1.0 \leq S/H \leq 4.0$). This study is motivated by the increasing use of compact heat exchangers in industry.

2. Numerical Investigation

When two series of fins are placed on the respective walls of a channel, flow is expected to reach a periodic fully developed regime, where the velocity field repeats itself from module to module, after a short entrance region [1, 2]. It is, therefore, possible to calculate the flow and heat transfer in a typical module such as ABCD shown in fig. 1, without the need for the entrance region calculation. The computational domain of numerical investigation is designated in fig. 1. The fins with fin height *F* are placed uniformly at a pitch *L* in each fin series. Thickness of the fin *t* and channel height *H* are kept constant, and their values are 0.0015 m and 0.060 m, respectively. The values of other four parameters are varied in the following range: *S*/*H* = 1.0-4.0, *Pr* = 0.7 and 3.5, *Re* = 100-500, *F*/*H* = 0 and 0.10. Flow is assumed laminar at Re = 500; because Berner *et al*. [2] indicated that flow is laminar for the Reynolds number of 600. Thus, blockage ratio, *F/H*, changes from 0 (smooth channel) to 0.10.

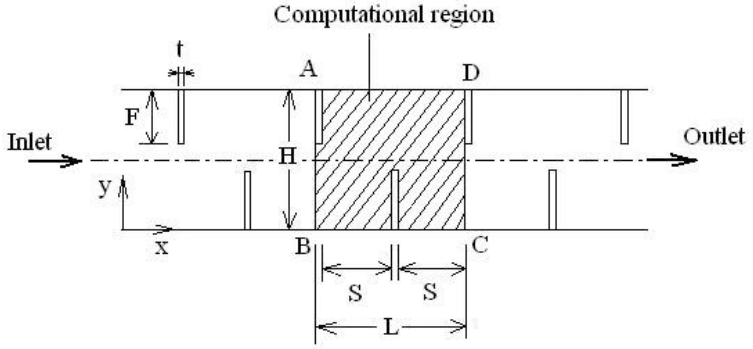

Figure 1. The computational model of the problem.

Numerical solutions are obtained using commercial software ANSYS Fluent 6.3.26. Air (*Pr* ≅ 0.7) and Freon-12 (*Pr* ≅ 3.5) are used as working fluid.

The continuity, momentum, and energy equations in Cartesian coordinate system for two dimensional, steady, incompressible, Newtonian, constant properties, and periodically fully developed laminar viscous flow of a fluid with negligible body forces, viscous dissipation, and radiation heat transfer are given as

$$\frac{\partial u}{\partial x}+\frac{\partial v}{\partial y}=0 \tag{1}$$

$$u\frac{\partial u}{\partial x}+v\frac{\partial u}{\partial y}=-\frac{1}{\rho}\frac{\partial p}{\partial x}+\upsilon\left(\frac{\partial^2 u}{\partial x^2}+\frac{\partial^2 u}{\partial y^2}\right) \tag{2a}$$

$$u\frac{\partial v}{\partial x}+v\frac{\partial v}{\partial y}=-\frac{1}{\rho}\frac{\partial p}{\partial y}+\upsilon\left(\frac{\partial^2 v}{\partial x^2}+\frac{\partial^2 v}{\partial y^2}\right) \tag{2b}$$

$$u\frac{\partial T}{\partial x}+v\frac{\partial T}{\partial y}=\alpha\left(\frac{\partial^2 T}{\partial x^2}+\frac{\partial^2 T}{\partial y^2}\right) \tag{3}$$

Boundary conditions are needed to solve the equations given above. The velocity components *u* and *v* in a periodically fully-developed flow can be written with

$$u(x,y)=u(x+L,y) \tag{4}$$

$$v(x,y)=v(x+L,y) \tag{5}$$

The pressure is expressed by

$$p(x,y)=-\beta x+\bar{p}(x,y) \tag{6}$$

where, the quantity $\bar{p}(x,y)$ is evaluated as

$$\bar{p}(x,y)=\bar{p}(x+L,y) \tag{7}$$

The inlet and outlet temperature boundary conditions can be written as

$$\frac{T(x,y)-T_{\mathrm{w}}}{T_{\mathrm{b}}(x)-T_{\mathrm{w}}}=\frac{T(x+L,y)-T_{\mathrm{w}}}{T_{\mathrm{b}}(x+L)-T_{\mathrm{w}}} \tag{8}$$

where

$$T_b(x) = \iint uTdA \Big/ \iint udA \tag{9}$$

Equations (4), (5), (7), and (8) describe the inlet and outlet boundary conditions. Constant heat flux ($\dot{q}''_w$ = 40 Wm^{-2}) and no-slip boundary conditions are used on the fin surfaces and channel walls, i.e.,

$$u = 0, \quad v = 0, \quad \partial T/\partial n = -\dot{q}''_w \Big/ k \tag{10}$$

Non-dimensional Reynolds number, average Nusselt number, and average Darcy friction factor are defined as

$$\mathrm{Re} = \rho U_o D_h / \mu \tag{11}$$

$$Nu_m = h_m D_h / k \tag{12}$$

$$f_m = 2(\Delta p / \rho U_o^2)(D_h / L) \tag{13}$$

Average convective heat transfer coefficient can be evaluated as shown in Eq. (14):

$$h_m = \dot{q}''_w \Big/ \left(T_w - (T_i + T_o)/2\right) \tag{14}$$

where T_w is evaluated as $T_w = \frac{1}{A}\int TdA$.

In order to compare the performance of all configurations tested, the results are given with thermal enhancement factor [20-23]:

$$\eta = \left(Nu_m / Nu_o\right) / \left(f_m / f_o\right)^{1/3} \tag{15}$$

The physical properties of the fluid are assumed to remain constant and taken at the bulk temperature of 300K [24].

2.1. Computational method

In this study, a general purpose finite-volume based commercial CFD software package ANSYS Fluent 6.3.26 has been used to carry out the numerical study. The code provides mesh flexibility by structured and unstructured meshes.

Computations are performed for laminar flow conditions. The energy equation is solved neglecting radiation as well as viscous dissipation effects. Quadrilateral cells are created with a fine mesh near the walls in Gambit 2.3. A non-uniform grid distribution was employed. Typical grid distribution in the vicinity of fin and channel wall is depicted in fig. 2. Close to each wall and fin surfaces, the number of grid points or control volumes are increased to enhance the resolution and accuracy. This is done to provide a sufficiently clustered mesh near the duct walls and to avoid sudden distortion and skewness.

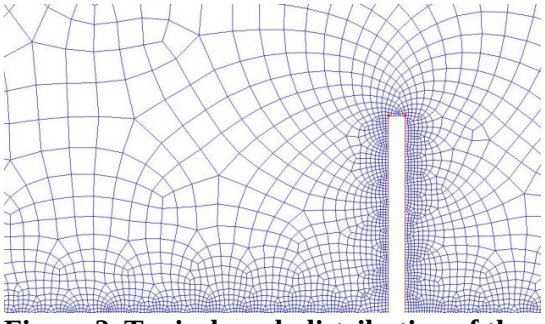

Figure 2. Typical mesh distribution of the computational domain.

The grid independence study is performed for all computational studies by refining the grid size until the variation in both the average Nusselt number and the average Darcy friction factor are less than 0.7%. Typical variation of the average Nusselt number and the average Darcy friction factor with mesh size is given in fig. 3 for S/H = 2.0, F/H = 0.10, Re = 500 and Pr = 0.7. Nine grid systems are tested in order to investigate the grid size effect for S/H = 2.0, F/H = 0.10, Re = 500 and Pr = 0.7. Grid sizes are changed from 789 to 24,377. It is seen that the increase of grid number from 12,286 to 24,377 has no significant effect in the calculated values of average Nusselt number and average Darcy

friction factor. Therefore, grid size is assumed to be fixed and equal to 12,286 for S/H = 2.0, F/H = 0.10, Re = 500 and Pr = 0.7. For other parameters analyzed here, the grid independence study is obtained in a similar manner.

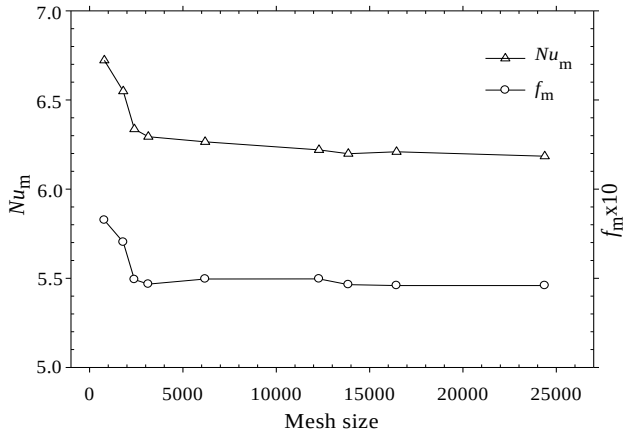

Figure 3. Variation of average Nusselt number and average Darcy friction factor with mesh size.

Steady segregated solver is used with second order upwind scheme for convective terms in the mass, momentum and energy equations. For pressure discretization, the standard scheme is employed while the SIMPLE-algorithm is used for pressure-velocity coupling discretization. No convergence problems are observed. To obtain convergence, each equation for mass, momentum and energy is iterated until the residual falls below 1×10^{-6}.

3. Results and Discussion

Variation of average Nusselt number and average Darcy friction factor with distance between two fins, Reynolds number, and Prandtl number has been investigated numerically. Numerical results obtained under steady-state conditions are presented in figs. 4-16.

Before presenting the new results, it is appropriate to validate the solution procedure to ascertain the accuracy and reliability of the flow and heat transfer results. For this purpose, the numerical computation is carried out for air flowing in a parallel plate channel at F/H = 0.10 and S/H = 2.0 for Re = 200. The result of this computation is compared with the result of Kelkar and Patankar [5] and Cheng and Huang [7] shown in tab. 1. It is seen that the present numerical result for Darcy friction factor is in good agreement with the literature.

Table 1. Comparison of numerical result with literature.

	Present study	Kelkar and Patankar [5]	Cheng and Huang [7]
$f_mRe/(fRe)_o$	1.23	1.2	1.2

Comparison of the x-velocity profile of this present study and the results of Cheng and Huang [7] is given in fig. 4 in the fully developed flow for F/H = 0 (i.e. smooth channel) at Re = 100. Figure 4 shows that the results of present study are in good agreement with those of Chen and Huang [7].

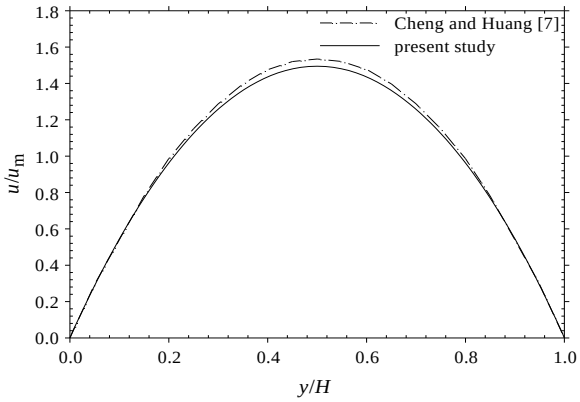

Figure 4. *x*-velocity profile in the fully developed flow for *F*/*H* = 0

The typical velocity and temperature distributions of air flow in duct for different Reynolds numbers are given in figs. 5 and 6, respectively, for *S*/*H*=1.0. It is obtained that velocity magnitudes increase with increasing Reynolds number; however, increasing Reynolds number decreases the magnitudes of the local temperature at a point in a channel. As can be seen in fig. 5, velocity field is affected due to presence of fin.

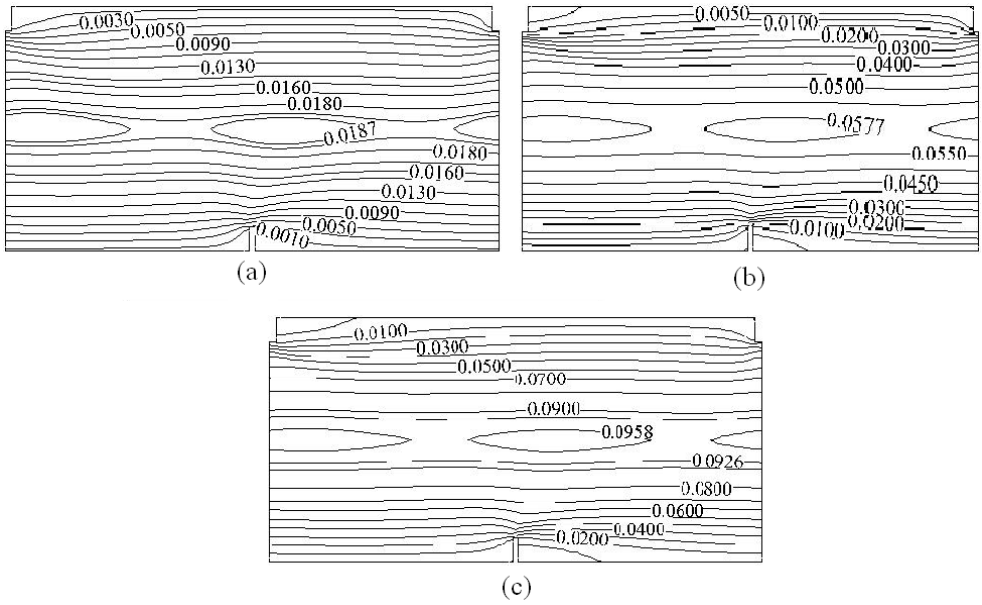

Figure 5. Velocity distribution for air flow in duct (a) *Re*=100, (b) *Re*=300, (c) *Re*=500.

The temperature distribution in duct at *Re* = 500 for flow of air (*Pr* ≅ 0.7) and Freon-12 (*Pr* ≅ 3.5) is given in figs. 7*a* and 7*b*, respectively, for *S*/*H*=1.0. It is seen in the figure that the temperature distribution in duct changes with changing working fluid.

Figure 8 shows the typical streamline profiles of the air flow in the computational domain for different Reynolds numbers at *S*/*H*=1.0. After the flow enters the channel, it separates from fin tip, and recirculation area occurs after fin. It is seen that large recirculation region occurs as Reynolds number increases. Thus, the reattachment point moves away from fin, on the bottom wall, when Reynolds number increases. Also, the strength of the recirculation flow increases with increasing Reynolds number. As can be seen in fig. 8, flow is deflected due to fins but do not impinge upon opposite wall.

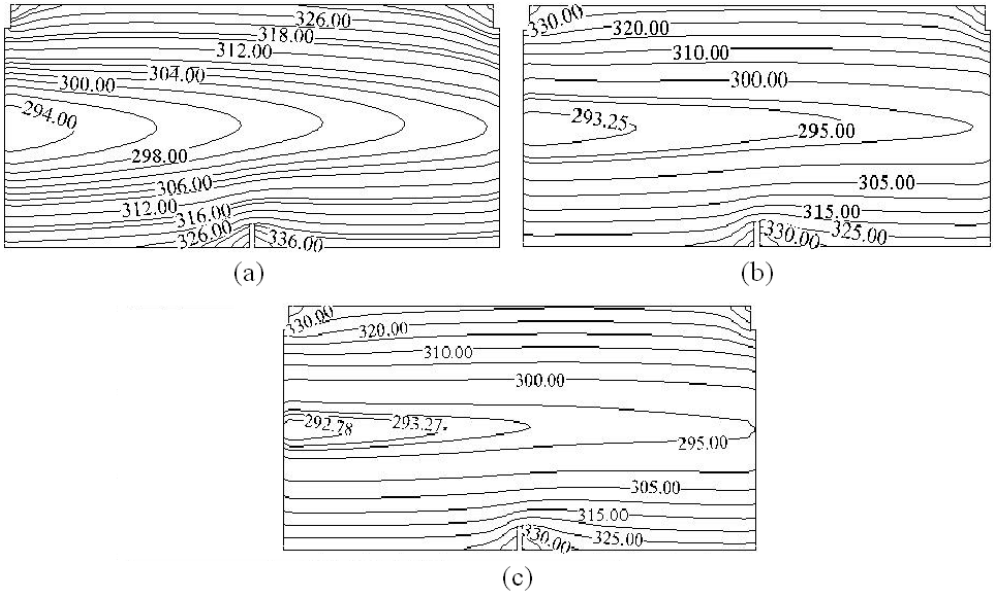

Figure 6. Temperature distribution for air flow in duct (a) *Re*=100, (b) *Re*=300, (c) *Re*=500.

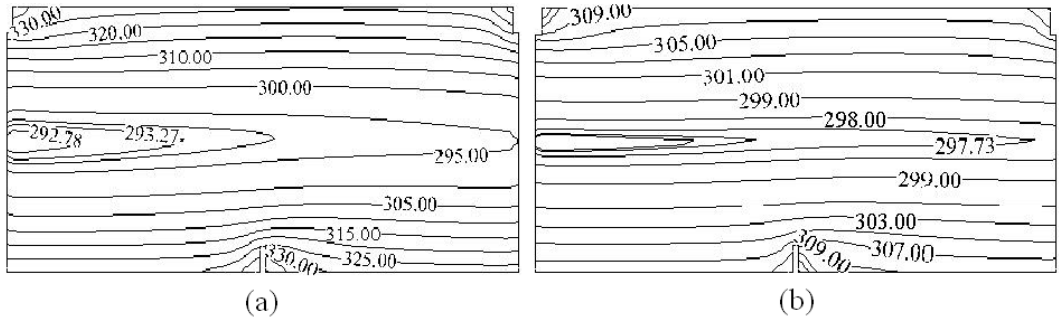

Figure 7. Temperature distribution at *Re*=500 for air (a) and Freon-12 (b).

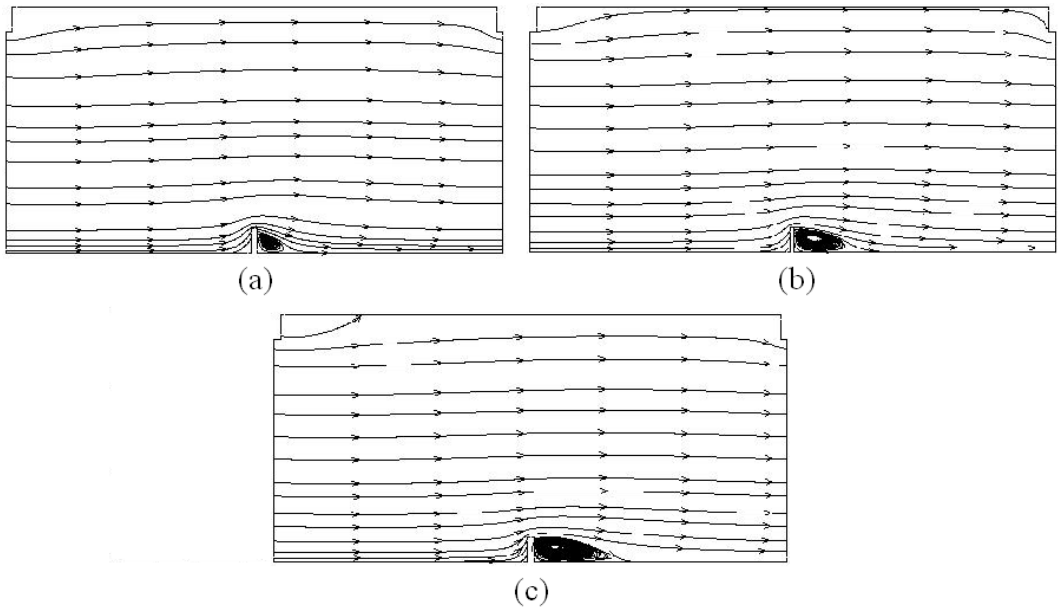

Figure 8. Streamline profiles of the air flow in the duct (a) *Re*=100, (b) *Re*=300, (c) *Re*=500.

The results of the computations are given in figs. 9 and 10 in terms of the ratios Nu_m/Nu_o and $f_mRe/(fRe)_o$ where the subscript "o" refers to the unfinned parallel plate channel. The values of Nu_o and $(fRe)_o$ are 8.23 and 96, respectively [24].

The normalized average Nusselt number is plotted in figs. 9*a* and 9*b* as a function of Reynolds number at different *S*/*H* for air and Freon-12, respectively. It is seen that increasing the distance between the two fins increases heat transfer. Nusselt number increases 20 and 16% as *S*/*H* changes from 1.0 to 4.0 for air and Freon-12, respectively. As the fin distance increases, the behavior approaches that in a finless channel. In other words, Nu_m/Nu_o approaches unity. As can be seen in fig. 9, Nu_m/Nu_o is less than unity. It is also seen that the ratios Nu_m/Nu_o slightly decreases as Reynolds number increases. This result agrees with the results of Kelkar and Patankar [5] and Tehrani and Abadi [12]. It can be interpreted as that fins with *F*/*H* = 0.10 do not have important effect to inflict flow on the opposite walls (please see fig. 8). The length of the recirculation region increases as Reynolds number increases (please see fig. 8). That is, direct contact between fluid and wall decreases as Reynolds number increases. Thus, decreased direct contact length results in low heat transfer.

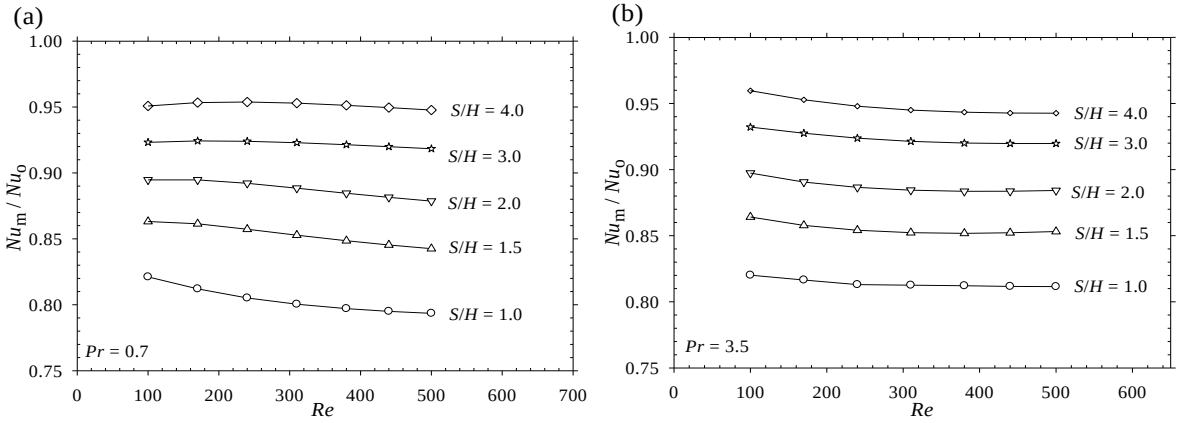

Figure 9. Variation of normalized average Nusselt number with Reynolds number for different *S*/*H* (a) *Pr* = 0.7, (b) *Pr* = 3.5.

The normalized average Darcy friction factor as a function of Reynolds number is sketched in figs. 10*a* and 10*b* at different *S*/*H* for air and Freon-12, respectively. As can be seen from figs. 10*a* and 10*b*, increasing the distance between the two fins decreases the friction factor at a given Reynolds number. In other words, closer spacing causes higher pressure drop. It is also seen that the ratios $f_mRe/(fRe)_o$ increases as Reynolds number increases. On average, friction factor decreases 24% as *S*/*H* changes from 1.0 to 4.0 for both air and Freon-12. As can be seen in fig. 10, as the fin distance becomes large, the behavior approaches that in a finless channel. That is, $f_mRe/(fRe)_o$ approaches unity.

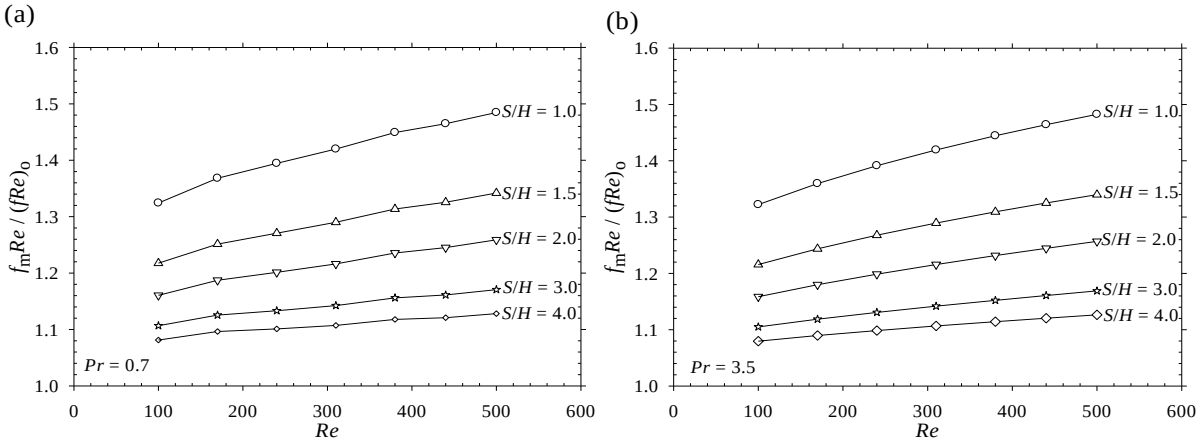

Figure 10. Variation of normalized average Darcy friction factor with Reynolds number for different *S*/*H* (a) *Pr* = 0.7, (b) *Pr* = 3.5.

Typical average Nusselt number as a function of fin distance is presented in fig. 11*a* at *Re* = 100 for *Pr* = 0.7 and *Pr* = 3.5. As shown in fig. 11a, the average Nusselt number for *Pr* = 3.5 is higher than that of *Pr* = 0.7 at a given fin distance. It is seen that as the fin distance becomes large, the behavior

approaches that in a finless channel. In other words, the value of Nu_m/Nu_o approaches unity. The phenomenon is similar to that observed by Kelkar and Patankar [5].

Figure 11*b* shows the normalized average Darcy friction factor as a function of fin distance at *Re* = 100 for *Pr* = 0.7 and *Pr* = 3.5. As shown in fig. 11*b*, Prandtl number does not affect the friction factor. It is also seen that friction factor decreases with increasing distance between two fins. In other words, as the distance between two fins increases, the result approaches the result of finless channel; that is, $f_m Re/(fRe)_o$ approaches unity. This result is similar to that observed by Kelkar and Patankar [5] and Garg *et al*. [18].

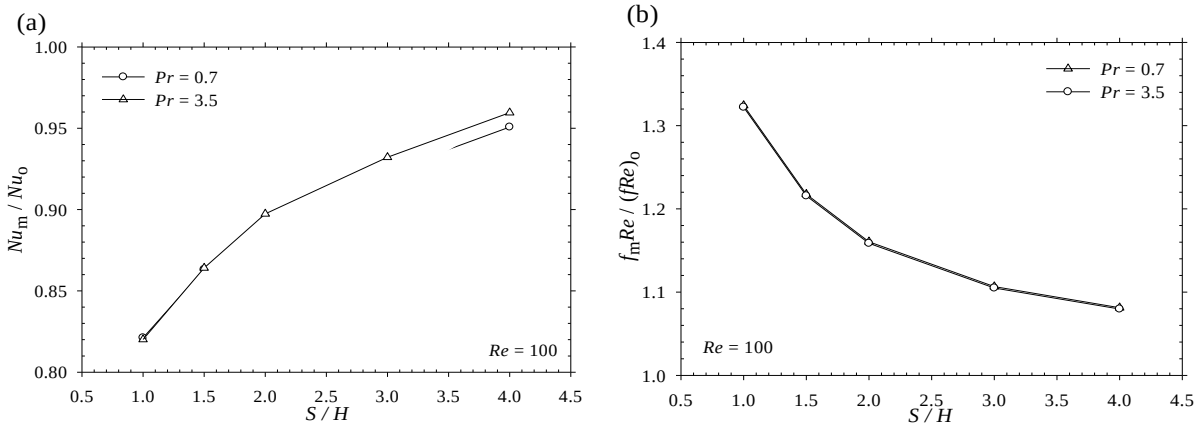

Figure 11. Variation of normalized average Nusselt number (a) and average Darcy friction factor (b) with fin distance.

Effect of Prandtl number on heat transfer and friction is shown in figs. 12*a* and 12*b*, respectively, for *S*/*H*=1.0. Attention now is focused to the fig. 12*a*. It is observed that average Nusselt number for Freon-12 (*Pr* ≅ 3.5) is higher than the average Nusselt number for air (*Pr* ≅ 0.7). As for the friction factor, it is seen from fig. 12*b* that average Darcy friction factor is the same for both air and Freon-12. It is also seen that average Darcy friction factor increases while the Reynolds number increases.

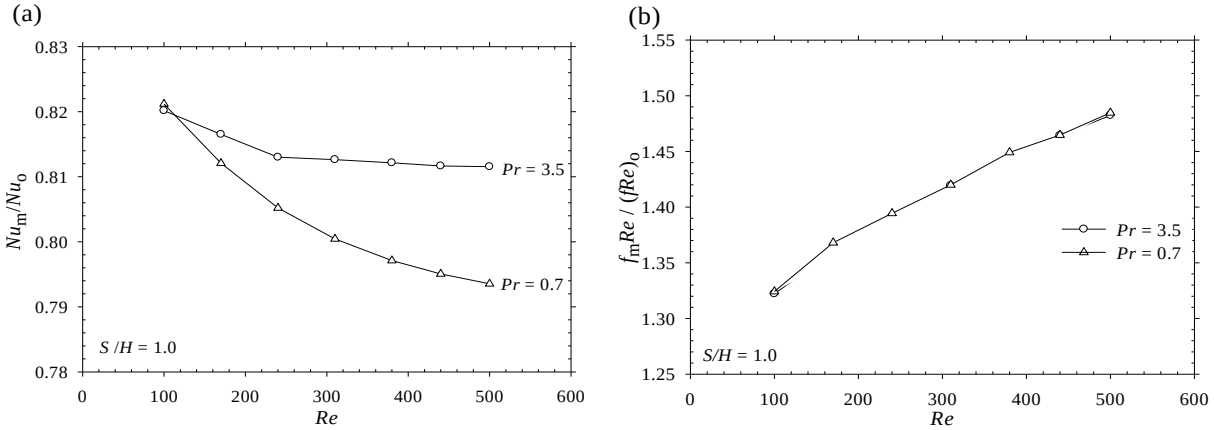

Figure 12. Variation of normalized average Nusselt number (a) and average Darcy friction factor (b) with Reynolds number for two different Prandtl numbers.

Thermal enhancement factors of the configuration for different *S*/*H* are shown as a function of Reynolds number in figs. 13*a* and 13*b* for air and Freon-12, respectively. It is seen that thermal enhancement factor of the configuration increases with the increasing distance between two fins for a constant Reynolds number. It can be explained that heat transfer dominates the friction while distance between two fins increases at a constant Reynolds number. It is also seen that thermal enhancement factor of the configuration slightly decreases as the Reynolds number increases. In other words,

friction dominates the heat transfer as the Reynolds number increases at constant *S*/*H*. As can also be seen from fig. 13, as the fin distance increases, thermal enhancement factor approaches the finless channel for which $\eta = 1$. It is also seen that the enhancement factor for all *S/H* is below unity. This indicates that this blockage ratio, *F/H* = 0.10, is not advantageous in comparison to smooth channel without fins in periodically fully developed laminar flow. This result agrees with that of Promvonge *et al*. [25]. Promvonge *et al*. [25] concluded that enhancement factor for the 90^o baffle indicates a decrease trend for blockage ratio less than or equal to 0.2.

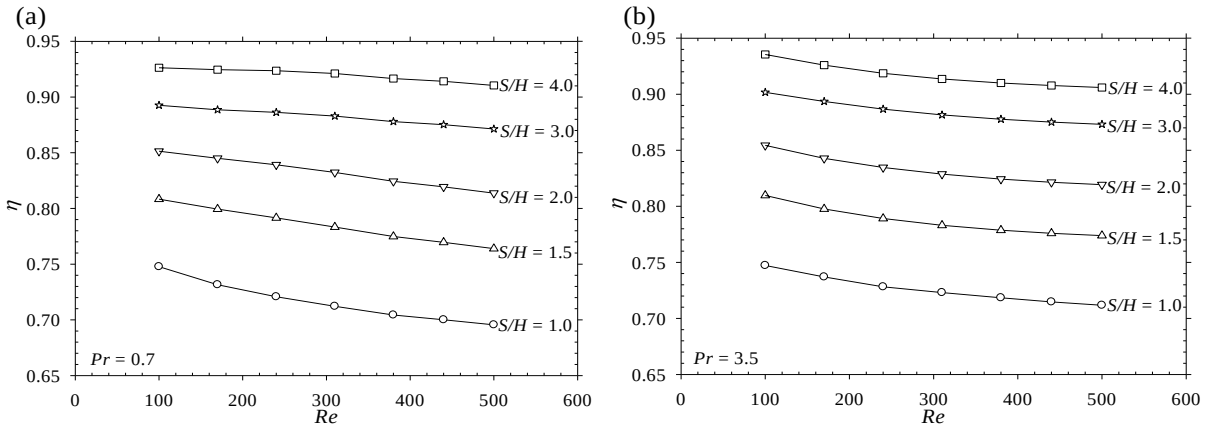

Figure 13. Variation of thermal enhancement factors of the configuration with Reynolds number for (a) *Pr* = 0.7, (b) *Pr* = 3.5.

In order to see the thermal enhancement factor of the configuration with two different Prandtl numbers, thermal enhancement factors of the configuration are depicted as a function of Reynolds number in fig. 14 for *S*/*H* = 1.0. It is seen that thermal enhancement factor of the configuration is higher for *Pr* = 3.5 than *Pr* = 0.7. That is, it can be said that heat transfer dominates the friction while the Prandtl number increases from *Pr* = 0.7 to 3.5 at constant Reynolds number.

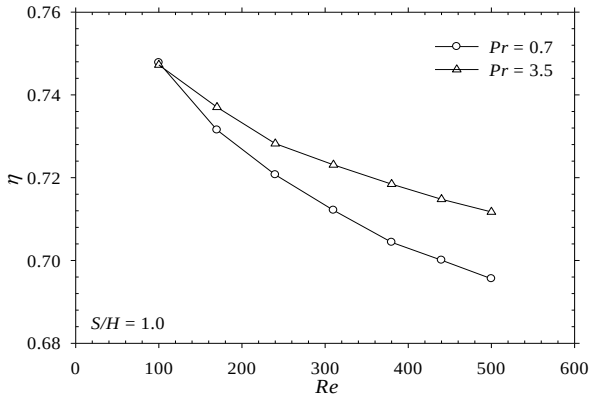

Figure 14. Variation of thermal enhancement factor of the configuration with Reynolds number for air and Freon-12.

Typical dimensionless axial velocity profiles u/U_o for air are plotted along channel height in fig. 15 at x = 0.002 m distance after the fin on the bottom wall for *S/H* = 1.0 at *Re* = 100 and 500. Axial velocity values are scaled to the inlet velocity. The negative velocities indicate the presence of recirculation behind the fin on the bottom wall. It is seen from inset (fig. 15) that the intensity of reverse flow increases with increasing Reynolds number, thus reverse flow with high intensity results in high pressure loss and high friction factor. This conclusion can also be seen in fig. 8.

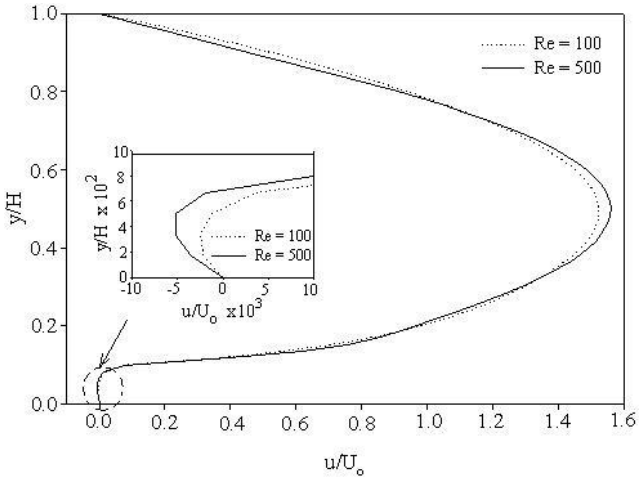

Figure 15. Typical dimensionless axial velocity profiles after the fin on the bottom wall for air at *Re* = 100 and *Re* = 500.

The variation of dimensionless reattachment length x_{rl}/H, evaluated from after the bottom baffle in the flow direction, with Reynolds number is shown in fig. 16 for S/H = 1.0. It is seen that the reattachment length increases as Reynolds number increases. This result can also be seen from fig. 8.

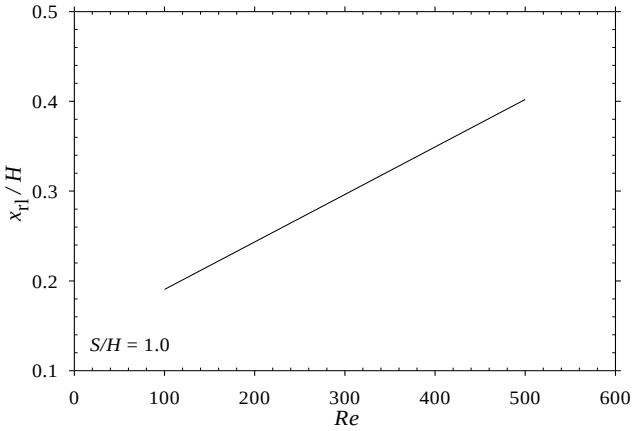

Figure 16. Reattachment length versus Reynolds number

4. Conclusions

In this study, two-dimensional laminar fluid flow and heat transfer characteristics between two horizontal parallel plates with staggered fins are investigated numerically under periodically fully developed conditions. ANSYS Fluent 6.3.26 commercial code is used in this investigation. Constant heat flux boundary condition is applied on the surfaces of the channel and fins. Study is implemented for one fin height (F/H = 0.10) and the special case of finless state (F/H = 0), different Reynolds numbers (Re = 100-500), Prandtl numbers (Pr = 0.7 and 3.5), and different distances between two fins (S/H = 1.0-4.0). It is obtained that heat transfer in the channel slightly decreases with increasing Reynolds number, but it increases with increasing fin distance for the blockage ratio of 0.10 in two dimensional periodically fully developed laminar flow. It is also seen that heat transfer in the channel for Pr = 3.5 is higher than that of Pr = 0.7. Friction factor increases with increasing Reynolds number; however, it decreases with increasing fin distance. It is seen that friction factor is the same for both air and Freon-12. Thermal enhancement factor of the configuration increases with fin distance and with the range of investigated Prandtl number, but slightly decreases with Reynolds number. It is concluded that fins having blockage ratio of 0.10 in two dimensional periodically fully developed laminar flow is not advantageous in comparison to smooth channel without fins.

Nomenclature

D_h – hydraulic diameter ($D_h = 2H$), [m]
F – fin height, [m]
f_m – average Darcy friction factor
f_o – average Darcy friction factor in finless duct
H – channel height, [m]
h_m – average convective heat transfer coefficient, [W·m^{-2}·K^{-1}]
L – length of the periodic zone, [m]
Nu_m – average Nusselt number
Nu_o – average Nusselt number in finless duct
p – fluid pressure, [Pa]
Δp – pressure loss, [Pa]
$\overline{p}$ – periodic variation term, [Pa]
Pr – Prandtl number
$\dot{q}''_w$ – heat flux, [W·m^{-2}]
Re – Reynolds number
xrl – reattachment length [m]
S – distance between two staggered fins, [m]
T – temperature, [K]
T_b – bulk temperature, [K]
T_i – inlet temperature, [K]
T_o – outlet temperature, [K]
T_w – wall temperature of the duct, [K]
t – fin thickness, [m]
u, v – the velocity components in x- and y-coordinates, [m·s^{-1}]
U_o – inlet velocity magnitude, [m·s^{-1}]
x, y – Cartesian coordinates

Greek symbols

α – thermal diffusion coefficient, [m^2·s^{-1}]
β – global pressure gradient, [Pa·m^{-1}]
η – thermal enhancement factor
υ – kinematic viscosity, [m^2·s^{-1}]
ρ – density, [kg·m^{-3}]

5. References

[1] Patankar, S. V., Liu, C. H., Sparrow, E. M., Fully Developed Flow and Heat Transfer in Ducts Having Streamwise Periodic Variation of Cross-Sectional Area, *Journal of Heat Transfer, 99* (1977), pp. 180-186
[2] Berner, C., *et al.*, Flow Around Baffles, *Journal of Heat Transfer, 106* (1984), pp. 743-749
[3] Shah, R. K., London, A. L., Laminar Flow Forced Convection in Ducts, in: *Advances in Heat Transfer* (Eds. T. F. Irvine, J. P. Hartnett), Academic Press, New York, USA, 1978
[4] Webb, B. W., Ramadhyani, S., Conjugate Heat Transfer in a Channel with Staggered Ribs, *International Journal of Heat and Mass Transfer*, *28* (1985), pp. 1679-1687
[5] Kelkar, K. M., Patankar, S. V., Numerical Prediction of Flow and Heat Transfer in a Parallel Plate Channel with Staggered Fins, *Journal of Heat Transfer, 109* (1987), pp. 25-30
[6] Lazaridis, A., Heat Transfer Correlation for Flow in a Parallel Plate Channel with Staggered Fins, *Journal of Heat Transfer, 110* (1988), pp. 801-802
[7] Cheng, C. H., Huang, W. H., Numerical Prediction for Laminar Forced Convection in Parallel-Plate Channels with Transverse Fin Array, *International Journal of Heat and Mass Transfer, 34* (1991), 11, pp. 2739-2749
[8] Luy, C. D., *et al.*, Forced Convection in Parallel-Plate Channels with a Series of Fins Mounted on the Wall, *Applied Energy*, *39* (1991), pp. 127-144

[9] Kim, S. H., Anand, N. K., Laminar Developing Flow and Heat Transfer between Series of Parallel Plates with Surface-Mounted Discrete Heat Sources. *International Journal of Heat and Mass Transfer, 37* (1994), 15, pp. 2231-2244
[10] Wang, G., *et al.*, Unsteady Heat Transfer in Baffled Channels, *Journal of Heat Transfer, 118* (1996), pp. 585-591
[11] Yuan, Z. X., *et al.*, Numerical Prediction for Laminar Forced Convection Heat Transfer in Parallel-Plate Channels with Streamwise-Periodic Rod Disturbances, *International Journal of Numerical Methods of Fluids*, *28* (1998), pp. 1371-1387
[12] Tehrani, F. B., Abadi, M. N., Numerical Analysis of Laminar Heat Transfer in Entrance Region of a Horizontal Channel with Transverse Fins, *International Communication of Heat and Mass Transfer, 31* (2004), 2, pp. 211-220
[13] Mousavi, S. S., Hooman, K., Heat and Fluid Flow in Entrance Region of a Channel with Staggered Baffles, *Energy Conversion and Management*, *47* (2006), pp. 2011-2019
[14] Onur, N., *et al.*, Numerical Investigation of the Effect of Baffles, Placed Between Two Parallel Plates on Flow and Heat Transfer Under Condition of Laminar Forced Convection, *Journal of Thermal of Science and Technology*, *27* (2007), 2, pp. 7-13
[15] Sripattanapipat, P., Promvonge, P., Numerical Analysis of Laminar Heat Transfer in a Channel with Diamond-Shaped Baffles, *International Communication of Heat and Mass Transfer*, *36* (2009), 1, pp. 32-38
[16] Turan, B., Oztop, H. F., Analysis of Heat Transfer in a Heated Tube with a Different Typed Disc Insertion, *Thermal Science*, *16* (2012), 1, pp. 139-149
[17] Xia, H. H., *et al.*, Simulation of Heat Transfer Enhancement by Longitudinal Vortex Generators in Dimple Heat Exchangers, *Energy*, *74* (2014), pp. 27-36
[18] Garg A., *et al.*, CFD Analysis of Laminar Heat Transfer in a Channel Provided with Baffles: Comparative Study between Two Models of Baffles: Diamond-Shaped Baffles of Different Angle and Rectangle, *International Journal of Enhanced Research in Science Technology & Engineering*, *3* (2014), 7, pp. 267-276
[19] Turgut, O., Kizilirmak, E., Effects of Reynolds Number, Baffle Angle, and Baffle Distance on Three-Dimensional Turbulent Flow and Heat Transfer in a Circular Pipe, *Thermal Science*, DOI. 10.2298/TSCI121011045T
[20] Valencia, A., *et al.*, Numerical Study of the Unsteady Flow and Heat Transfer in Channels with Periodically Mounted Square Bars, *Heat and Mass Transfer*, *37* (2001), 2-3, pp. 265-270
[21] Kore, S. S., *et al.*, Experimental Investigations of Heat Transfer Enhancement from Dimpled Surface in a Channel, *International Journal of Engineering Science and Technology*, *3* (2011). 8, pp. 6227-6234
[22] Promvonge, P., *et al.*, Numerical Heat Transfer Study of Turbulent Square-Duct Flow Through Inline V-Shaped Discrete Ribs, *International Communications in Heat and Mass Transfer*, *38* (2011), 10, pp. 1392-1399
[23] Potdar, U., *et al.*, Study of Heat Transfer Coefficient & Friction Factor of Stationary Square Channel with V Shaped 45^{o} Angled Arc of Circle Ribs with Different Blokage Ratio, *International Journal of Applied Sciences and Engineering Research*, *1* (2012), 2, pp. 47-56
[24] Bergman, T. L., *et al.*, *Fundamentals of Heat and Mass Transfer,* 7^{th} Ed., John Wiley & Sons Inc., New York, USA, 2011
[25] Promvonge, P., *et al.*, Numerical Investigation of Laminar Heat Transfer in a Square Channel with 45^{o} Inclined Baffles, *International Communications in Heat and Mass Transfer*, *37* (2010), pp. 170-177